

Magnetic Field Disturbance Produced by Electric Railway

By

KAZUO YANAGIHARA

Nagoya Local Meteorological Observatory

Abstract: Leakage currents of electric railway may give serious disturbance to magnetic observation at a nearby observatory. A method of estimating the amount of disturbance is studied.

1. Introduction

DC electric railway is one of the major sources of disturbance to natural magnetic field observation. The rails, a part of electric circuit of railway, having contact with the earth for a very long distance produce a wide distribution of leakage electric current which causes a considerable magnetic field over wide area. If AC power is used for railway, there may be no disturbance to ordinary magnetic observation even at a site very near to the railway, because ordinary instruments used in magnetic observation are insensitive to AC field. In this paper, magnetic field disturbances produced by simplified DC railway systems are calculated, and then, verified by field observations. The troubles caused by AC field in electronic instruments will not be discussed here. Actual electric systems of a railway is of course more complicated, but the present method of estimation should be useful for them.

2. Magnetic Field Produced by Electric Railway

The current of electric railway is supplied from power substation(s) to the feeder and trolley wire and returned through the rail after driving the motors of electric car (the load). The feeder and trolley wire will be referred to as feeder hereafter. If the rail is well insulated from the earth, the current simply flows through elongated rectangular circuit whose long sides are the feeder and rail. The effect of magnetic field produced by the current in this insulated circuit may be negligible for our purposes. However, insulation of rail is usually not so good, and the amount of leakage current could be as much as some tens of

percent of the total load current. Magnetic field produced by this leakage current is a source of serious artificial disturbance for natural magnetic field observation even if a magnetic observatory is situated some ten kilometres away from the railway.

The leakage current at a point on the earth's surface will disperse as it enters the earth, but the magnetic field of the dispersing currents measured at a distant point on the earth's surface is the same as the magnetic field produced by a semi-infinite vertical line current of the same total amount if the earth is homogeneous with a constant electrical resistivity. Leakage current $i(s)ds$ from a small segment ds of rail s at a point S produces a horizontal magnetic field, $\vec{Z}_0 \times \vec{r} \cdot i(s)ds/r^2$, at a point P on the earth's surface, where \vec{Z}_0 is the vertical downward unit vector and \vec{r} is the position vector \vec{SP} (Fig. 1).

On the other hand a horizontal current $J(s)$ at S produces a vertical magnetic field, $\vec{ds} \times \vec{r} \cdot J(s)/r^3$, at P . When r is much larger than the height of the feeder, horizontal current $J(s)$ is the sum of feeder current I and rail current $J_r(s)$,

$$J(s) = I + J_r(s) \quad (1)$$

where I and $J_r(s)$ are positive when flowing towards the positive direction of s . If I is positive, $J_r(s)$ is negative. And $J_r(s)$ is related to the leakage current density $i(s)$ by

$$i(s) = -\frac{dJ_r(s)}{ds} \quad (2)$$

Total magnetic field \vec{H} at P is given by

$$\vec{H} = \int_L \frac{\vec{Z}_0 \times \vec{r}}{r^2} i(s) ds + \int_L \frac{\vec{ds} \times \vec{r}}{r^3} J(s) \quad (3)$$

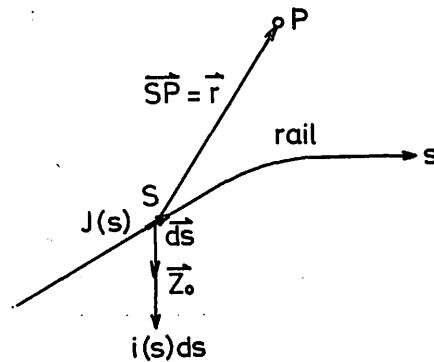


Fig. 1. Leakage current $i(s)ds$ and horizontal current $J(s)$ of railway s and position vector \vec{r} .

where integrations should be done for range L of s in which $i(s)$ or $J(s)$ exists. Hereafter, magnetic field implies that caused by the railway.

Distributions of $i(s)$ and $J(s)$ are determined by the electrical circuit of railway. When $i(s)$ and $J(s)$ are known, \vec{H} can be calculated by Eq. (3) for the homogeneous earth.

3. Rail Current Distribution

Letting R be rail resistance per unit length and η be leakage resistance for unit length, electrical potential $V(s)$ of the rail is given by

$$V(s) = \eta i(s) \tag{4}$$

and relates to $J_r(s)$ by

$$\frac{dV(s)}{ds} = -R J_r(s) \tag{5}$$

With Eqs. (2), (4) and (5), rail current $J_r(s)$ is determined by

$$\frac{d^2 J_r(s)}{ds^2} = \frac{R}{\eta} J_r(s) \tag{6}$$

which gives

$$J_r(s) = Ae^{\alpha s} + Be^{-\alpha s} \tag{7}$$

where

$$\alpha = \sqrt{R/\eta} \tag{8}$$

and the constants A and B are determined by boundary conditions. In Fig. 2, current I is supplied from a single power substation at $s=0$ to a single load at $s=l$ (>0) and the rail is terminated (or insulated) at $s=-l_1$ and $s=l_3=l+l_2$ ($l_1, l_2 > 0$). At both ends of the rail, rail currents are zero, i. e.,

$$J_r(-l_1) = J_r(l+l_2) = 0 \tag{9 a}$$

and at the other boundaries, $s=0$ and l , rail currents are denoted by

$$J_r(0_-) = I + J_r(0_+) = I_1 \quad \text{and} \quad I + J_r(l_-) = J_r(l_+) = I_2 \tag{9 b}$$

respectively, where subscripts $-$ and $+$ mean those at negative side and positive side in the s -coordinate respectively. With boundary currents thus defined, $J_r(s)$

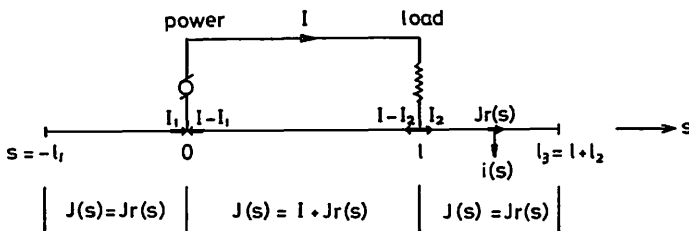


Fig. 2. A simplified electric circuit of railway.

for the simplified circuit of Fig. 2 is given by

$$J_r(s) = \begin{cases} I_1 \sinh \alpha(s+l_1)/\sinh \alpha l_1 & \text{for } -l_1 \leq s \leq 0 \\ -\{(I-I_1) \sinh \alpha(l-s) \\ + (I-I_2) \sinh \alpha s\}/\sinh \alpha l & 0 \leq s \leq l \\ I_2 \sinh \alpha(L+l_2-s)/\sinh \alpha l_2 & l \leq s \leq l+l_2 \end{cases} \quad \begin{matrix} (10 a) \\ (10 b) \\ (10 c) \end{matrix}$$

At boundaries $s=0$ and $s=l$, electrical potential $V(s)$ calculated from the rail current of one side should be the same as that of the other side.

This gives

$$I_1/\tanh \alpha l_1 = (I-I_1)/\tanh \alpha l - (I-I_2)/\sinh \alpha l \quad (11 a)$$

and
$$I_2/\tanh \alpha l_2 = -(I-I_1)/\sinh \alpha l + (I-I_2)/\tanh \alpha l \quad (11 b)$$

from which rail currents at boundary,

$$I_1 = \frac{1+(T-S)T_2}{1+T(T_1+T_2)+T_1T_2} I \quad (12 a)$$

$$I_2 = \frac{1+(T-S)T_1}{1+T(T_1+T_2)+T_1T_2} I \quad (12 b)$$

are obtained, where

$$S=1/\sinh \alpha l, \quad T=1/\tanh \alpha l, \quad T_1=1/\tanh \alpha l_1, \quad T_2=1/\tanh \alpha l_2 \quad (13)$$

With typical values of rail resistance $R=0.0088$ ohm/km and leakage resistance $\eta=0.5$ ohm·km, I_1 and I_2 for the two circuits shown in Fig. 3 are as follows.

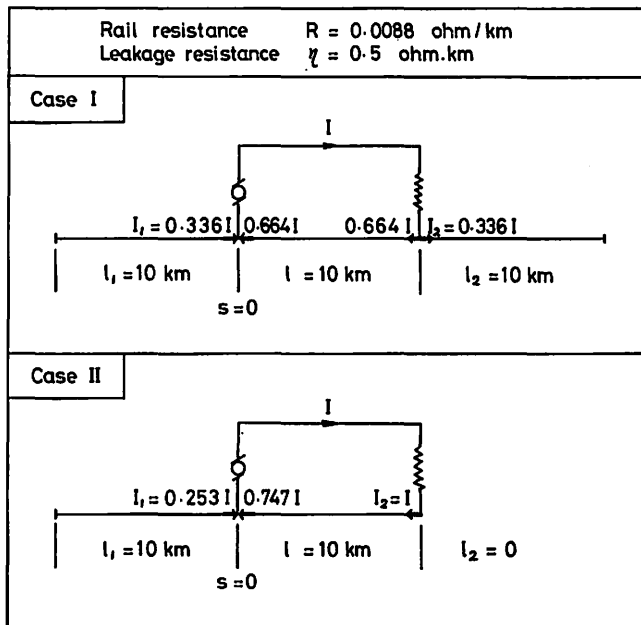


Fig. 3. Case I and Case II of simplified circuit.

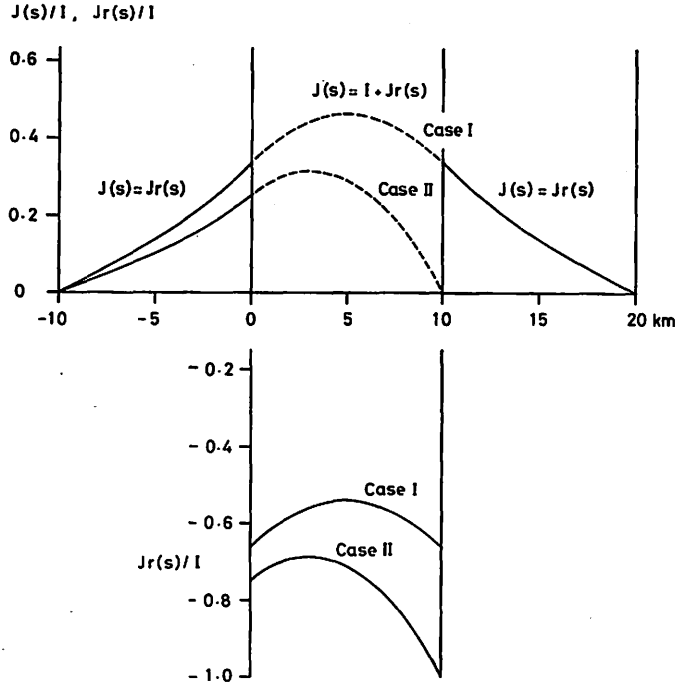


Fig. 4. Rail current $J_r(s)$ and horizontal current $J(s)$ of Case I and Case II.

$$I_1 = I_2 = 0.336 I \quad \text{for Case I} \quad (14)$$

$$I_1 = 0.253 I \quad \text{and} \quad I_2 = 0 \quad \text{for Case II} \quad (15)$$

Case I means $l = l_1 = l_2 = 10$ km, and Case II means $l = l_1 = 10$ km and $l_2 = 0$. When I_1 and I_2 are known, rail current $J_r(s)$ can be calculated by Eqs. (10 a), (10 b) and (10 c). Fig. 4 shows $J_r(s)$ by full line for Case I and Case II. Broken lines of the figure show horizontal current $J(s) = I + J_r(s)$ for a segment $0 \leq s \leq l$. For the other segments $-l \leq s \leq 0$ and $l \leq s \leq 2l$, $J(s)$ is equal to $J_r(s)$ because $I = 0$.

4. Magnetic Field Calculation

In calculating magnetic field by Eq. (3), it is convenient to use an approximate expression of rail current:

$$J_r(s) = a + bs + cs^2 \quad (16)$$

where a , b and c are constants determined so as to minimize the error for a given segment of railway. For the segment $0 \leq s \leq l$ of Fig. 2, the constants may be determined on the condition that Eq. (16) gives exact values of rail currents at boundaries $s = 0$ and $s = l$ and that it gives exact extreme value (minimum in absolute value) of rail current at a point between the two boundaries given by

$$J_m = -(I - I_1) / \cosh[\tanh^{-1}\{T - S(I - I_2) / (I - I_1)\}] \quad (17)$$

With J_m , I_1 and I_2 given, constants a , b and c are

$$\left. \begin{aligned} a &= -(I - I_1) \\ b &= 2\{I - I_1 + J_m + \sqrt{(I - I_1 + J_m)(I - I_2 + J_m)}\} / l \\ c &= -\{2I - I_1 - I_2 + 2J_m + 2\sqrt{(I - I_1 + J_m)(I - I_2 + J_m)}\} / l^2 \end{aligned} \right\} \quad \text{for } 0 \leq s \leq l \quad (18 a)$$

For the segment $-l_1 \leq s \leq 0$, the last condition—the exact extreme value at a point between two boundaries—is changed to the exact value of potential at $s = -l_1$ because rail current decreases monotonically towards the negative s direction. This and the other two conditions—exact value at boundaries—determine constants a , b and c , as

$$\left. \begin{aligned} a &= I_1 \\ b &= \{2 - \alpha l_1 / \sinh \alpha l_1\} I_1 / l_1 \\ c &= \{1 - \alpha l_1 / \sinh \alpha l_1\} I_1 / l_1^2 \end{aligned} \right\} \quad \text{for } -l_1 \leq s \leq 0 \quad (18 b)$$

Similarly for the segment $l \leq s \leq l + l_2$, the same expressions of a , b and c are obtained by use of l_2 for l_1 and I_2 for I_1 , provided that the origin of s is shifted to l and the direction of s is reversed.

For Case I, approximate expressions of rail current are

$$J_r(s) = \begin{cases} \{0.336 + 0.418(s/l) + 0.082(s/l)^2\} I & \text{for } -l \leq s \leq 0 & (19 a) \\ \{-0.664 + 0.496(s/l) - 0.496(s/l)^2\} I & 0 \leq s \leq l & (19 b) \\ \{0.336 + 0.418\left(\frac{l-s}{l}\right) + 0.082\left(\frac{l-s}{l}\right)^2\} I & l \leq s \leq 2l & (19 c) \end{cases}$$

($l = 10$ km)

and for Case II

$$J_r(s) = \begin{cases} \{0.253 + 0.314(s/l) + 0.061(s/l)^2\} I & \text{for } -l \leq s \leq 0 & (20 a) \\ \{-0.747 + 0.390(s/l) - 0.643(s/l)^2\} I & 0 \leq s \leq l & (20 b) \end{cases}$$

($l = 10$ km)

These approximate values of rail current are so close to exact values given by Eq. (10) that discrimination in Fig. 4 is, even if plotted, almost impossible.

If s is a straight line and rail current is given by Eq. (16), integration in Eq. (3) will be easy. Taking a Cartesian coordinate system (x , y , z) whose x -axis is the straight line of railway with positive direction towards the flow of feeder current I and whose z -axis is the downward vertical (Fig. 5), magnetic field \vec{H} at P (0 , p , 0) on y -axis is given by

$$H_x = \sum_i \left\{ b_i \tan^{-1} \frac{p(v_i - u_i)}{p^2 + u_i v_i} + c_i p \log \frac{p^2 + v_i^2}{p^2 + u_i^2} \right\} \quad (21 a)$$

$$H_y = \sum_i \left\{ \frac{b_i}{2} \log \frac{p^2 + v_i^2}{p^2 + u_i^2} + 2c_i \left(v_i - u_i - p \tan^{-1} \frac{p(v_i - u_i)}{p^2 + u_i v_i} \right) \right\} \quad (21 b)$$

$$H_z = \sum_i \left\{ \frac{I + a_i - c_i p^2}{p} \left(\frac{v_i}{\sqrt{p^2 + v_i^2}} - \frac{u_i}{\sqrt{p^2 + u_i^2}} \right) - b_i p \left(\frac{1}{\sqrt{p^2 + v_i^2}} - \frac{1}{\sqrt{p^2 + u_i^2}} \right) + c_i p \log \frac{v_i + \sqrt{p^2 + v_i^2}}{u_i + \sqrt{p^2 + u_i^2}} \right\} \quad (21 c)$$

where a_i , b_i and c_i are constants in an approximate expression of rail current

$$J_r(x) = a_i + b_i x + c_i x^2 \quad (22)$$

for the i -th segment, $u_i \leq x \leq v_i$, of the rail, and I should be zero for the segments without feeder current.

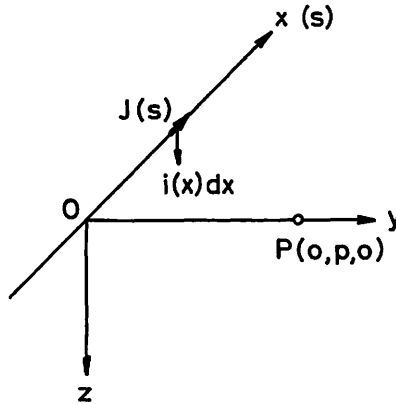


Fig. 5. Cartesian coordinate system (x, y, z) for a straight line railway s , for homogeneous earth.

The magnetic field due to any curvilinear portion may be obtained as the sum of contributions from straight segments.

Considering a case that a railway passes by a magnetic observatory (Case I_p of Fig. 6), origin O of the coordinate system (x, y, z) is taken at $s=l/2$ of Case I. With variable s replaced by $x + (l/2)$ in Eqs. (19 a), (19 b) and (19 c),

$$J_r(x) = a_i + b_i x + c_i x^2 \quad \text{for } u_i \leq x \leq v_i$$

$$= \begin{cases} \{0.566 + 0.500(x/l) + 0.082(x/l)^2\}I & \text{for } -3/2 \leq (x/l) \leq -1/2 & (23 a) \\ \{-0.540 - 0.496(x/l)^2\}I & -1/2 \leq (x/l) \leq 1/2 & (23 b) \\ \{0.566 - 0.500(x/l) + 0.082(x/l)^2\}I & 1/2 \leq (x/l) \leq 3/2 & (23 c) \end{cases}$$

$(l = 10 \text{ km})$

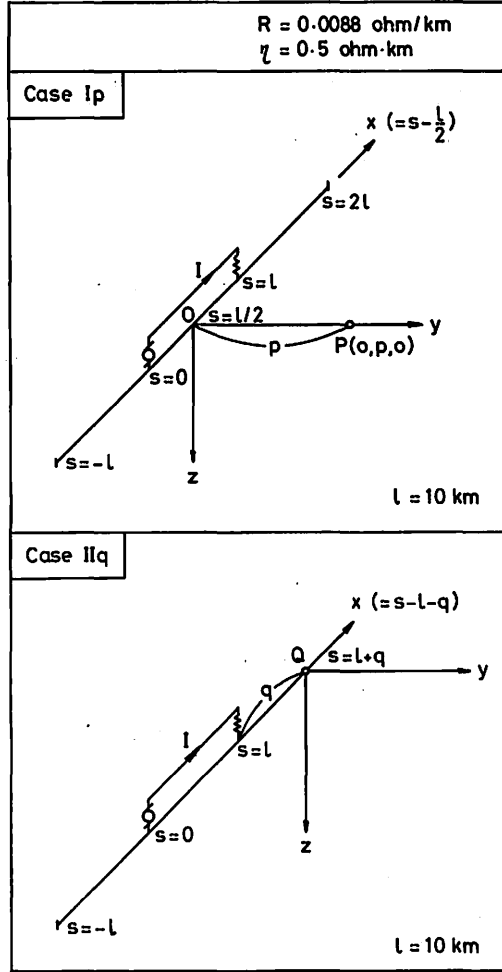


Fig. 6. Case I_p and Case II_q, for homogeneous earth.

Substituting the values of a_i , b_i , c_i , u_i and v_i given by Eqs. (23 a), (23 b) and (23 c) into Eqs. (21 a), (21 b) and (21 c), the magnetic field at P (0, p , 0) is given by

$$H_x(I_p) = 0 \tag{24 a}$$

$$\begin{aligned}
 H_y(I_p) = & \left[0.500 \log \frac{(p/l)^2 + (1/2)^2}{(p/l)^2 + (3/2)^2} \right. \\
 & + 0.328 \left\{ 1 - \frac{p}{l} \tan^{-1} \frac{p/l}{(p/l)^2 + (3/4)} \right\} \\
 & \left. - 0.992 \left\{ 1 - \frac{p}{l} \tan^{-1} \frac{p/l}{(p/l)^2 - (1/4)} \right\} \right] \frac{I}{l} \tag{24 b}
 \end{aligned}$$

$$\begin{aligned}
 H_z(I_p) = & \left[-\frac{0.106 + 0.422(p/l)^2}{(p/l)\sqrt{(p/l)^2 + (1/2)^2}} + \frac{1.698 + 0.754(p/l)^2}{(p/l)\sqrt{(p/l)^2 + (3/2)^2}} \right. \\
 & + 0.164 \frac{p}{l} \log \frac{(3/2) + \sqrt{(p/l)^2 + (3/2)^2}}{(1/2) + \sqrt{(p/l)^2 + (1/2)^2}} \\
 & \left. - 0.496 \frac{p}{l} \log \frac{(1/2) + \sqrt{(p/l)^2 + (1/2)^2}}{-(1/2) + \sqrt{(p/l)^2 + (1/2)^2}} \right] \frac{I}{l}
 \end{aligned}
 \tag{24 c}$$

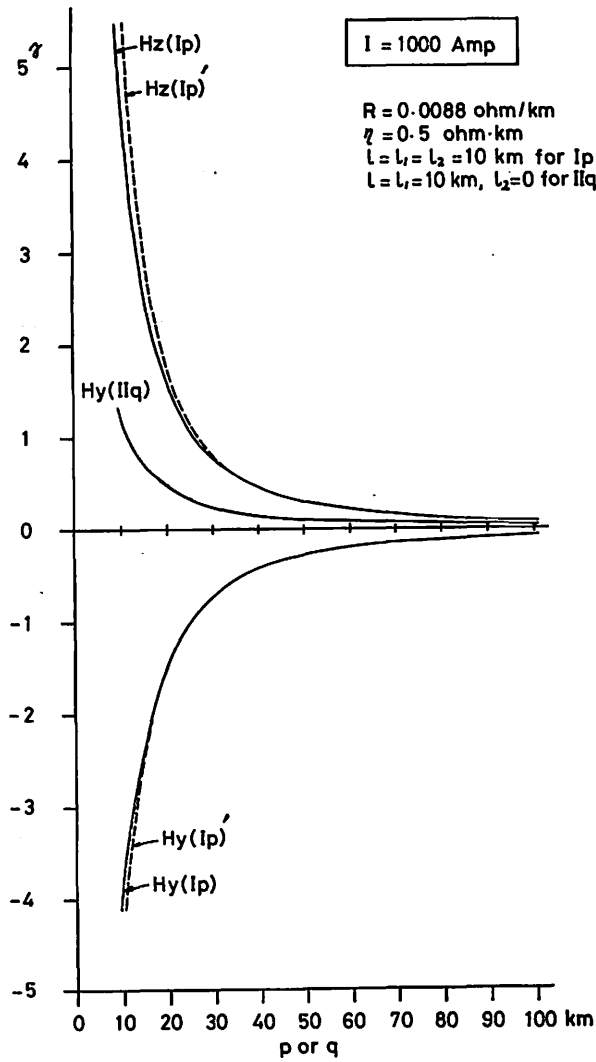


Fig. 7. Calculated magnetic field for Case I_p and Case I_q , for homogeneous earth.

For $I=1000$ amp, calculated values of magnetic field are shown by full lines in Fig. 7 for $p=10$ to 100 km.

When a railway is terminated at a distance of q from Q (Case II_q of Fig. 6) the magnetic field at Q is approximated by Case II of Fig. 3, with $s=l+q$. In this case it is convenient to use s -coordinate in calculation of magnetic field, though this is a special case of Eqs. (21 a), (21 b) and (21 c), with $p=0$. Using rail current $J_r(s)$ given in Eqs. (20 a) and (20 b), the magnetic field at Q is given by

$$H_x(\text{II}_q) = H_z(\text{II}_q) = 0 \quad (25 \text{ a})$$

$$\begin{aligned} H_y(\text{II}_q) &= \int_L^{l+q} \frac{1}{l+q-s} \frac{dJ_r(s)}{ds} ds \\ &= \left\{ \left(0.439 + 0.124 \frac{q}{l} \right) \log \frac{1+(q/l)}{2+(q/l)} \right. \\ &\quad \left. - \left(0.896 + 1.286 \frac{q}{l} \right) \log \frac{q/l}{1+(q/l)} - 1.164 \right\} \frac{I}{l} \end{aligned} \quad (25 \text{ b})$$

For $I=1000$ amp, calculated values of the magnetic field are shown in Fig. 7 for $q=10$ to 100 km.

All the magnetic field components shown in Fig. 7 decrease rapidly with distance p or q up to 30 or 40 km, and then the decrease is much slowed down.

5. Approximate Calculation for Distant Point

In case p or q is sufficiently larger than l , the leakage currents and their return currents widely distributed along the rails may be approximated, for calculation of horizontal magnetic field, by a downward concentrated vertical current and an upward one, respectively, where each of the two concentrated currents is equivalent in strength to the respective set of currents and is located at the centre of distribution.

For Case I_p, the total amount of leakage current is $I+J_m=0.460 I$ and the point of assumed concentration is $x=0.74 l$ (Fig. 8). The total amount of return current is the same $0.460 I$, with direction of flow the opposite of leakage current and the point of concentration at $x=-0.74 l$. These two vertical line currents produce a magnetic field

$$H_y(I_p)' = -0.681 (I/l) / \{0.74^2 + (p/l)^2\} \quad (l=10 \text{ km})$$

at P (0, p , 0). This, approximate value of $H_y(I_p)$, is shown by a broken line in Fig. 7.

Similarly for Case II_q, the downward vertical current $0.312 I$ at $s=0.8 l$ and upward one $-0.312 I$ at $s=-0.3 l$ give an approximate value of

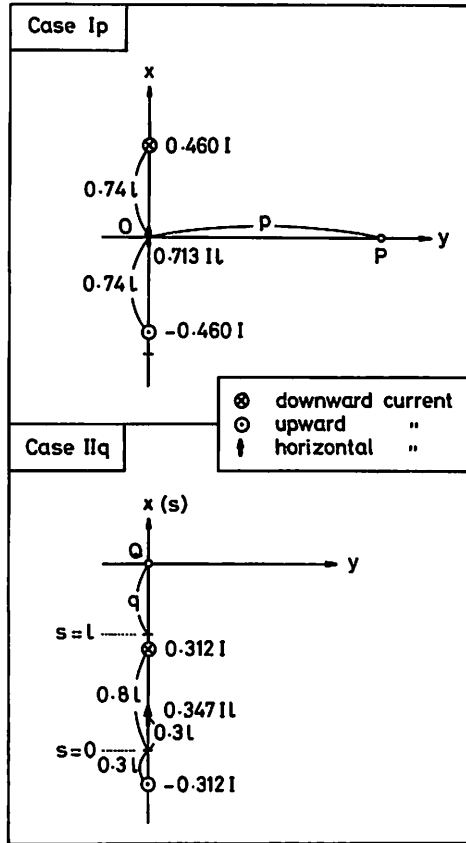


Fig. 8. Approximation of concentrated vertical and horizontal currents for a distant observation site.

$$H_y (II_q)' = 0.312 (I/l) [1/\{0.2 + (q/l)\} - 1/\{1.3 + (q/l)\}] \quad (l = 10 \text{ km})$$

for $H_y (II_q)$ at Q, or $s = q + l$. This value is so close to $H_y (II_q)$ for $q = 10$ to 100 km that discrimination in Fig. 7 is impossible.

Similar approximate calculation of vertical component of magnetic field at a distant point is made with an assumption that the entire horizontal current is concentrated, keeping integrated current moment $\int J(s) ds$ at a constant value, at a point where $|J(s)|$ is at a maximum. Being turned into a constant by this assumption, \vec{r} in Eq. (3) is replaced by a constant vector \vec{r}_0 which is \vec{r} at the point where $|J(s)|$ is at a maximum. For Case I_p , the maximum of $|J(s)|$ occurs at $s = (1/2)l$ which is origin O of (x, y, z) . Approximate value of $H_z (I_p)$ is given by

$$H_z(I_p)' = (1/p)^2 \int_{-l}^{2l} J(s) ds = (1/p)^2 \left\{ Il - \frac{2I_1}{\alpha \sinh \alpha l} \right\}$$

$$= 0.713 (Il) / (p/l)^2 \quad (l=10 \text{ km})$$

which is shown by a broken line in Fig. 7. For Case II_q, the maximum of $|J(s)|$ occurs at $s=0.3l$ and the concentrated horizontal current moment at this point is given by

$$\int_{-l}^l J(s) ds = Il \{ 1 - 2(I/I_1) / (\alpha l \sinh \alpha l) - 1 / (\alpha l \tanh \alpha l) + 1 / (\alpha l \sinh \alpha l) \} = 0.347 Il \quad (l=10 \text{ km}) \quad (26)$$

which causes no magnetic effect at Q ($s=l+q$), but this value will be used in the next section.

The foregoing approximate calculation indicates, as Fig. 7 implies, that the value of the magnetic field can be given by this approximate calculation with satisfactory accuracy for locations about 30km or more away from the railway.

6. Two-Substation System

According to an IAGA (International Association of Geomagnetism and Aeronomy) resolution, a magnetic observatory, if newly constructed, should be located more than 30km away from any electric railway. At 30km distance, our calculated values of magnetic field components are several tenths of γ , a bit larger than tolerable noise level in geomagnetic observation, even for a comparatively small load current of 1000 amp in a single power substation railway system, as is shown in Fig. 7. However, the magnetic field may be much weaker if the same load current is jointly supplied from two power substations situated on either sides of the load.

Any ordinary railway line has usually many power substations distributed along its length, and a load moving between two power substations is supplied with currents from both.

For this situation, the magnetic field is of course obtained by combining the contributions from each side of the load. Letting $2l=20$ km be the distance between two power substations with a load with current I at the centre, the feeder current and rail current on each side are one half of those of Case II, with the flow direction of one side opposite to that of the other side. With one power substation taken as origin O of coordinate system (x, y, z) in which x -axis coincides with the railway and z -axis is the downward vertical (Fig. 9), assumed concentrated vertical currents for approximate calculation of magnetic field at a distant point are $-0.312I/2$ at $x=-0.3l$ and $2.3l$, and $0.312I/2$ at

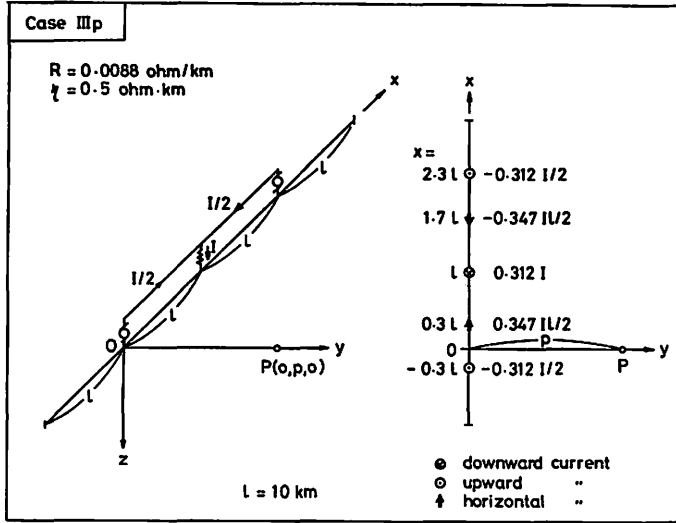


Fig. 9. Case III_p of two power substations, for homogeneous earth.

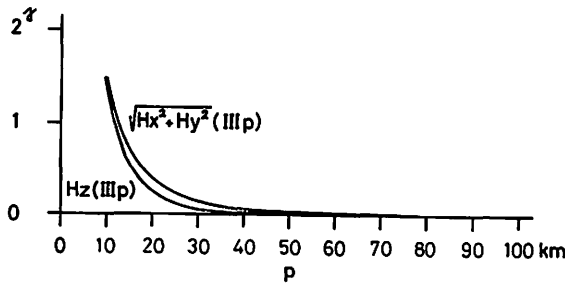


Fig. 10. Horizontal and vertical components of magnetic field for Case III_p of two power substations.

$x=0.8l$ and $1.2l$. The sum of the last two positive currents is equivalent to $0.312I$ at $x=l$. Assumed concentrated horizontal current moments are $0.347 Il/2$ at $x=0.3l$ and $-0.347 Il/2$ at $x=1.7l$. These concentrated currents produce a magnetic field \vec{H} (III_p) comprising

$$H_x(III_p) = \left\{ \frac{1}{2 \cdot 3^2 + (p/l)^2} - \frac{1}{0.3^2 + (p/l)^2} - \frac{2}{1 + (p/l)^2} \right\} \frac{p}{l} \cdot \frac{0.312}{2} \frac{I}{l}$$

$$H_y(III_p) = \left\{ \frac{2.3}{2 \cdot 3^2 + (p/l)^2} - \frac{0.3}{0.3^2 + (p/l)^2} - \frac{2}{1 + (p/l)^2} \right\} \frac{0.312}{2} \frac{I}{l}$$

$$H_z(III_p) = \left\{ \frac{1}{(\sqrt{0.3^2 + (p/l)^2})^3} - \frac{1}{(\sqrt{1.7^2 + (p/l)^2})^3} \right\} \frac{p}{l} \cdot \frac{0.347}{2} \frac{I}{l}$$

at P (0, p , 0) on y -axis. Fig. 10 shows calculated values of horizontal component $\sqrt{H_x^2 + H_y^2}$ (III_p) and vertical component H_z (III_p) for $I=1000$ amp. Both values are very small compared with those of Case I_p for a single power substation.

Though based on the assumption of a stationary load, the above-mentioned result indicates that a multi-substation system is good in reducing possible artificial magnetic disturbance. However, if either of the two power substations becomes out of order, the disturbance at the nearby observatory may shoot up.

The magnetic disturbance may further be reduced by making the distance between power substations shorter. Total amount of leakage current is smaller for smaller l . In order to show this relationship quantitatively, the total leakage current in an extreme case that l_1 and l_2 approach ∞ in the simplified circuit of Fig. 2 given by

$$\text{Maximum of } |J(s)| = I + J_m = \{1 - (1 + e^{-\alpha l}) / \cosh(\alpha l / 2)\} I \tag{27}$$

is calculated for different values of l , and shown in Fig. 11 for $\alpha=0.133$. At $l=10$ km, the amount of total leakage current is $0.483 I$ which is not so much different from $0.460 I$ of Case I whose l_1 and l_2 are both 10km. On the other hand, the amount changes considerably with l which is the distance between the load and power substation.

As Eq. (27) shows, the amount of total leakage current depends upon αl . Therefore α and l are of equal importance in reducing leakage current, while

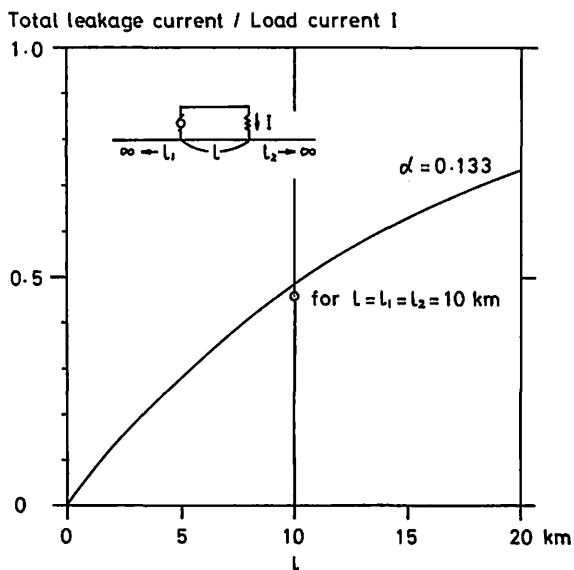


Fig. 11. Change in total leakage current with l .

rail resistance R and leakage resistance η , which determine the value of α by Eq. (8), contribute only by square root of their value.

7. Field Experiment and Discussions

With cooperation of Japan National Railway and Kakioka Magnetic Observatory, an organized experiment was carried out along the Jōban Line in 1954 when electrification of the railway line was planned for the portion which would affect our observatory. At the time, DC electrification of the Jōban Line had been completed from the Tokyo area to a point a few kilometres northeast of Abiko, marked by a double crossing in Fig. 12. A single crossing designated as "Intersection" a few kilometres down the line indicates the point where the DC line extended from the Tokyo area is terminated and AC line begins. The electric cars on the Jōban Line are compatible to both AC and DC. One area of experiment was the neighbourhood of existing power substations at Kanamachi and Abiko (Area A in Fig. 12) and the other was the neighbourhood of Kakioka, and Ishioka which is the nearest railway station to Kakioka (Area B).

In Area A, current was supplied from the Abiko power substation to dummy loads, one at Kanamachi and another near the middle point between Abiko and Kanamachi. Electric cars were not used because the load was desired to be at fixed locations. Experiments were carried out for several nights in small hours when regular electric car operations were at a rest.

Observed rail currents are expressed well by Eq. (10 b) for the segment between the load and power substation. Leakage coefficient α is obtained from the observed rail current distribution, but it is different for different days of experiment. The values of leakage resistance η calculated from α are 0.53, 0.55, 1.32, 1.40, 1.42 and 1.43 ohm·km for respective days of experiment, with the rail resistance corrected for temperature change. The first two η values are of snowing days and the rest are of clear days.

Rail currents are expressed approximately by Eq. (16) for the segment between the load and power substation, like Eq. (19 b) of Case I or Eq. (20 b) of Case II. For the other segments of monotonic decreasing current, approximate expression of rail current is $J_r(s) = I_1 \{(s/d) - 1\}^2$ with conditions $J_r(d) = 0$ and $J_r(0) = I_1$ in this experiment, slightly different from those for Case I and Case II. Here, d is a distance along the rail. Approximate expressions of rail current thus obtained from observed values as functions of coordinate s along the rail are used for calculation of magnetic field. Applying Eqs. (21 a), (21 b) and (21 c) for successive straight railway segments, expected magnetic field at observation

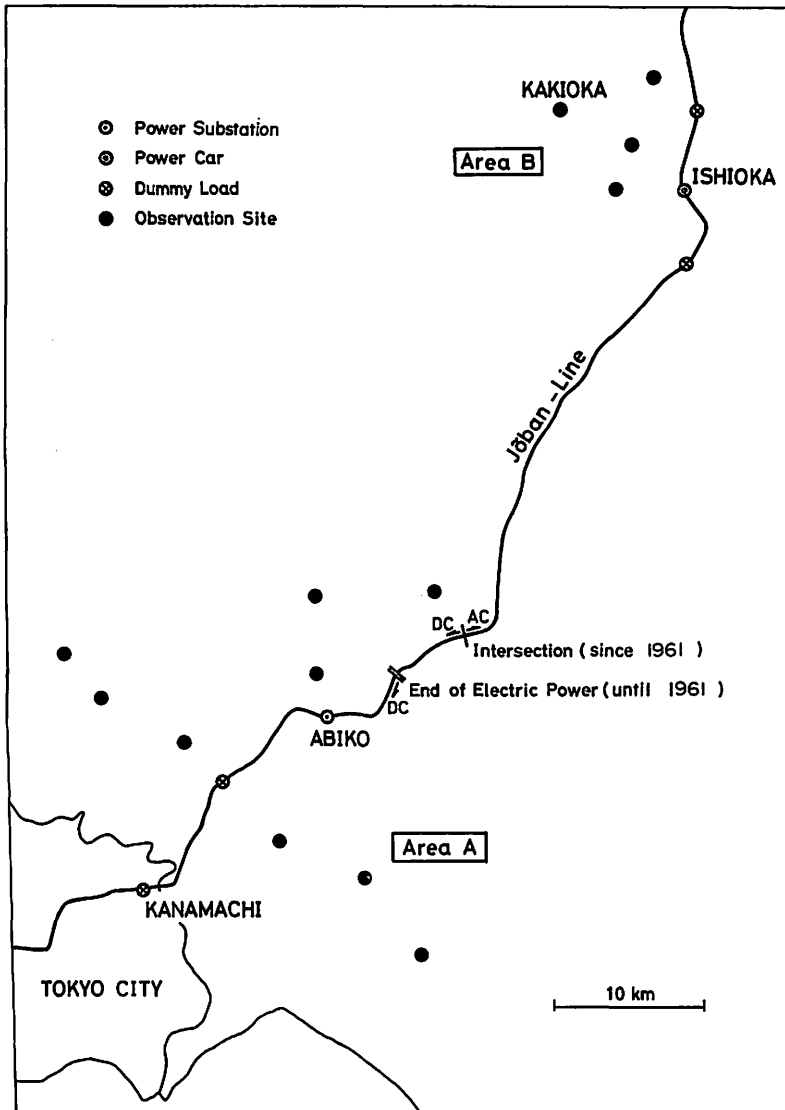


Fig. 12. Map of the area of field experiment.

site is calculated by summing up contributions from each segment.

Since the rails in Area B were not connected electrically, unlike those in Area A, at the time of our experiment, the return current through the rails could not be compared on equal terms between Areas A and B. Therefore, the dummy load was insulated from the rails and then connected to a ground rod

before measuring magnetic field. The same procedure was followed in the two areas for comparison. The magnetic field at observation site is calculated on the basis of one each concentrated vertical current at the sites of the dummy load and power substation, and a horizontal current between them.

For the experiment in Area B, a mobile power generator car parked at Ishioka was used since no other power source was available. A dummy load was placed 6.5 km south of Ishioka down the line and another 5.5 km to the north (Fig. 12). Current distribution to ground rods was varied and the number of combinations of relative current values came to six.

The artificial magnetic field was observed at 9 sites in Area A and 4 sites in Area B. Observed values of the magnetic field are not necessarily very close to the calculated values. Distribution of ratios of observed value to calculated one is shown in Fig. 13. For Area A, the number of ratio values is 36 which is the combination of 9 observation sites, 2 magnetic field components, $\sqrt{H_x^2 + H_y^2}$ and H_z , and 2 kinds of return circuits, the ground rod and rails. There is no measurable difference in ratio distribution between the 2 kinds of circuits. Though the mean of the 36 ratio values is very close to unity, they scatter rather widely. For Area B, the number of ratio values is 48 which is the combination of 4 observation sites, 2 magnetic field components, and 6 combinations of current distribution to ground rods. The mean of the 48 ratio values is much less than unity. But the range of distribution is similar to that of Area A except the one at 11.0 and another at -0.5 whose negative sign means the direction of observed

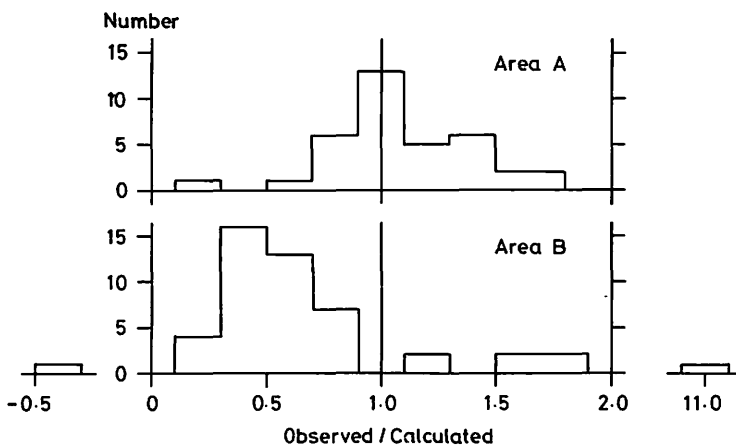


Fig. 13. Distribution of ratio of the observed magnetic field to the calculated one in our field experiment.

vertical component is the opposite to the calculated one.

The difference between observed and calculated values seems to be mainly due to non-uniformity of the earth resistivity in the area. Magnetic field calculations mentioned above are all based on homogeneous earth with a constant resistivity. It is rather difficult to map three-dimensional distribution of earth resistivity for the entire area involved, though this knowledge should be the basis of magnetic field calculation. If precise distribution is not known, calculated values for homogeneous earth should at least be doubled in estimating artificial disturbance, as inferred from Fig. 13.

If DC power was used for the railway in Area B, artificial magnetic field at Kakioka could have been higher than the tolerable noise level with the expected load of the railway even if leakage coefficient α and the distance between power substations were minimized by economically feasible way. However AC power has been employed in electrifying the railway soon after our experiment, so that there is no disturbance from the railway for observation of natural magnetic field at Kakioka.

In order to estimate or watch the disturbance caused by real railways of DC power, there are many other factors to be taken into consideration other than the simplified studies given above. For example, rails are sometimes connected to ground grid such as underground gas-pipe system, which increases local leakage current. Increase of leakage current is caused also by decrease of leakage resistance of the rail, which may be caused by soiling of the rails, sleepers, etc. in a long time. In a railway system involving a number of power substations, supply voltage from individual power substations could fluctuate, which, if occurred, would alter the current supply share among power substations.

電気鉄道の地磁気じょう乱

柳原 一夫

(名古屋地方気象台)

電気鉄道からの漏えい電流は広い範囲にわたって磁場をつくり、自然磁場測定に対して重大なじょう乱源となっている。地磁気観測所の観測障害対策のため、基本的構成の電気鉄道についてじょう乱磁場を計算した。